UCLA
UCLA Electronic Theses and Dissertations

Title
The Effects of Sex and Aging on Regional Grey Matter in the preclinical model of Multiple Sclerosis

Permalink
https://escholarship.org/uc/item/4dp9b20s

Author
Cortez-Delgado, Diego

Publication Date
2023

Peer reviewed|Thesis/dissertation

eScholarship.org Powered by the California Digital Library
University of California

UNIVERSITY OF CALIFORNIA

Los Angeles

The Effects of Sex and Aging on Regional Grey Matter in the preclinical model of Multiple Sclerosis

A thesis submitted in partial satisfaction of the requirements for the degree Master of Science in Physiological Science

by

Diego Cortez-Delgado

2023

© Copyright by

Diego Cortez-Delgado

2023

ABSTRACT OF THE THESIS

The Effects of Sex and Aging

on Regional Grey Matter

in the preclinical model of Multiple Sclerosis

by

Diego Cortez-Delgado

Master of Science in Physiological Science

University of California, Los Angeles, 2023

Professor Rhonda Voskuhl, Chair

Professor Art Arnold, Co-Chair

Professor Stephanie Correa, Co-Chair

Multiple Sclerosis (MS) is a heterogeneous disease that impacts the brain, spinal cord, and optic nerve. The etiology of MS is not completely understood, but the nature of these autoimmune inflammatory and neurodegenerative lesions has been under investigation for decades. Biological aging has been reported to be more than a significant factor associated with neurodegenerative diseases. Thalamic grey matter atrophy in MS has increasingly been demonstrated with normal aging, and a sexual dimorphism over time has been reported even at the earliest forms of the disease. The thalamus is a critical relay center, and the association of the thalamus in MS has been linked to various clinical symptoms ranging from vision loss, motor

deficits, cognitive impairment, numbness, and fatigue. Using the preclinical model of MS, experimental autoimmune encephalomyelitis (EAE), we assessed the neuropathology of thalamic grey matter and spinal cord white matter in sex-matched and age-matched wild-type mice to better understand the motor disability seen in MS and EAE. The experiment with healthy controls and EAE middle age and young mice revealed significant widespread microglia activation, astrocyte activation, and synaptic loss in aged mice. This neuropathology in the MS model during aging suggests that similar neuropathology may contribute to thalamic grey matter atrophy in progressive MS. The role of biological aging witnessed in thalamic network injury in EAE and MS related symptoms is key in highlighting the manifestation of variable lesions that are influenced by biological sex and aging.

The thesis of Diego Cortez-Delgado is approved

Art Arnold, Committee Co-Chair

Stephanie Correa, Committee Co-Chair

Rhonda Voskuhl, Committee Chair

University of California, Los Angeles

2023

Multiple Sclerosis (MS) is a complex disease involving the central nervous system (CNS) and the immune system. The process of myelin injury and axonal injury is a multifaceted process involving variable inflammation, demyelination, and can affect axonal loss throughout various regions in the CNS (Minagar, 2013; Smith and Garg, 2015). Depending on the location of lesions, clinical symptoms of MS can range from vision loss, motor deficits, pain, cognitive deficits, numbness, and tingling to name a few (Amin and Ontaneda, 2021; Capone, 2019). MS is multifactorial with symptoms appearing and subsiding over time. The differing clinical courses of MS can be classified as clinically isolated syndrome (CIS), relapsing-remitting multiple sclerosis (RRMS), primary progressive multiple sclerosis (PPMS), and secondary progressive multiple sclerosis (SPMS). A diagnosis of MS is based on the McDonald's diagnostic criteria that correlates patient disabilities with CNS lesions in magnetic resonance imaging (MRI), cerebrospinal fluid (CSF), and optical tests that help differentiate MS symptoms from other conditions with similar symptoms. There is significant heterogeneity between patients regarding which disability is most affected, and the rate of worsening of each disability differs even within the same patients. The Voskuhl laboratory has proposed that known regional differences in the brain at the cellular and molecular levels suggest that a "one size fits all" approach to understanding disability progression is insensitive. Instead, region specific investigations are needed to understand, and identify treatments optimized and tailored to prevent each disability (Voskuhl, 2019; Tassoni, 2019; Itoh, 2018).

As with other autoimmune diseases there is a higher prevalence of MS among women than men. MS affects women at a ratio of 3-to-1, but despite this female bias in disease susceptibility, men display more rapid disability progression (Voskuhl, 2012; Voskuhl, 2020;

Ortona, 2016). A previous cross-sectional study included MRI data from MS patients in an observational study at the NeuroCure Clinical Research Center at the Charité – Universitätsmedizin Berlin with imaging analyses done at the UCLA Dept. of Neurology. Sex differences in neurodegeneration by comparing deep grey matter volume in males and females with MS and their age- and sex-matched healthy controls. Voxel-based morphometry in MS men and women revealed significant worse regional gray matter atrophy in the thalamus when compared to their age-matched and sex-matched controls (Voskuhl, 2020). Additionally, thalamic volume strongly correlated with MS men performing worse on the 9-hole peg test than MS women, further establishing that male sex increases the risk for disability progression (Voskuhl, 2020). These stark clinical differences only begin to underscore the sex related differences in MS between men and women, as well as the effect of biological aging.

Animal studies in the experimental autoimmune encephalomyelitis (EAE) model for MS have demonstrated a similar increase in females to susceptibility to disease, due in part to having the XX sex chromosome complement in the immune system (Ortona, 2016; Voskuhl, 2012; Smith-Bouvier, 2008), while having XY in the CNS leads to worse neurodegeneration (Eshaghi, 2018; Du, 2014). Thalamic atrophy has been observed early in MS, with progressive spreading to the cerebral cortex later in disease (Bergsland, 2012; Eshaghi, 2018; Voskuhl, 2020). Additionally, progressive thalamic volume loss has been demonstrated in normal aging (Hughes, 2012) and a sexual dimorphism in thalamic atrophy over time has been reported (Voskuhl, 2020). Regional differences in grey matter atrophy have been shown in MS, additionally distinct disabilities are directly correlating with identifiable grey matter atrophy in selective CNS regions (Bakshi, 2001; Morgen, 2006; Prinster, 2010; MacKenzie-Graham, 2016). Using the preclinical model of MS, EAE, we investigated the age- and sex-related differences in thalamic atrophy

between young and midlife, male and female mice by comparing results of healthy and disease age- and sex-matched mice.

Results:

EAE induction and clinical scoring

EAE was induced in wild-type, GFAP-Cre: RiboTag, and NSE-Cre: RiboTag mice. EAE scores are taken immediately following disease induction. All mouse groups were monitored daily for EAE signs based on a standard EAE 0 to 5 scale scoring system as follows: 0, healthy; 1, complete loss of tail tonicity; 2, loss of righting reflex; 3, partial paralysis; 4, complete paralysis of one or both hind limbs; and 5, premoribund state. Clinical signs began around 11 days post induction. After scoring mice for 45 days post induction, we saw no sex differences in EAE walking scores between C57BL/6 males and females, as previously described by our lab and others (Figure 1). Also, as described by one previous report (Segal, 2022) both sexes revealed worse disability at midlife. The first round of EAE induction was performed in wild-type C57BL/6 mice. Both sexes showed worse EAE scores in midlife mice, but only males had a significant difference between age. The second round of EAE induction was done in a GFAP-Cre: RiboTag mouse line. Again, both sexes showed worse EAE scores at midlife with significant difference between ages. The third round of EAE induction was done in an NSE-Cre: RiboTag mouse line. Both males and females at midlife showed worse EAE scores, but only males had a significant age difference. In all groups, males repeatedly demonstrated statistically significant age differences in EAE scores between young and midlife mice consistent with the effect of aging on walking disability progression as seen in MS.

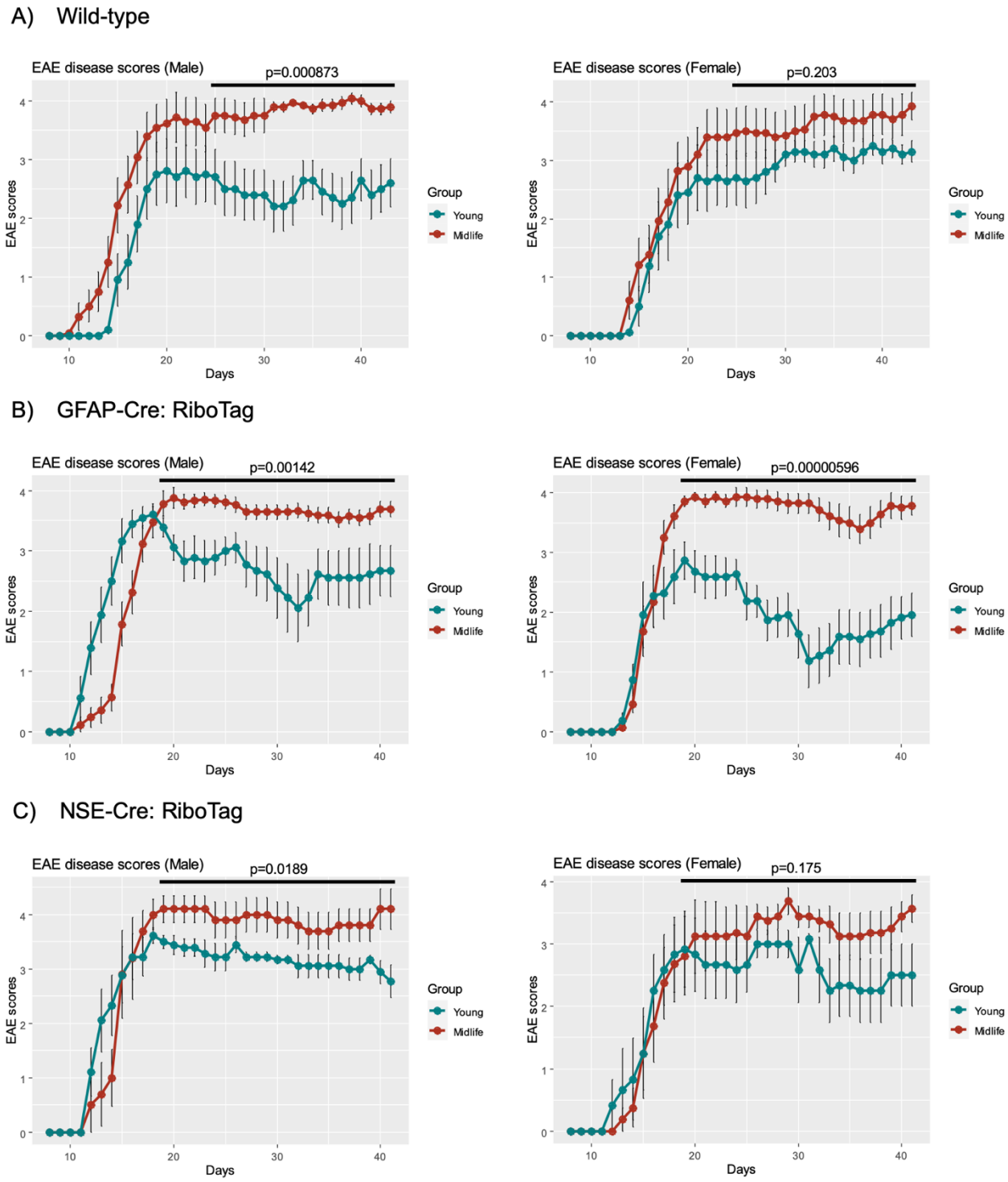

Figure 1: EAE clinical scoring. Male and female walking disability scores for days 0 – 45. (A) Wild-type male (left) and female (right) clinical scores grouped by age (n = 48; midlife male = 14, midlife female = 14, young male = 10, and young female = 10). (B) GFAP-Cre: RiboTag male (left) and female (right) clinical scores grouped by age (n = 50; midlife male = 21, midlife female = 14, young male = 9, young female = 11). (C) NSE-Cre: RiboTag male (left) and female (right) clinical scores grouped by age (n = 28; midlife male = 5, midlife female = 8, young male = 9, young female = 6). Daily scores are based on an average of all individual scores for that group.

Aged EAE mice had severe demyelination, axonal injury, and neuron loss in spinal cord

Spinal cord injury was assessed in male spinal cord between disease and healthy controls. Demyelination was determined by comparing the percent area of myelin basic protein (MBP) staining. Ventral spinal cord regions showed significant demyelination in midlife controls and midlife EAE when compared between ages. The dorsal spinal cord regions revealed a similar decrease in MBP positive area at midlife control and midlife EAE compared to young age, but there was also a significant decrease in MBP positive area in young EAE males. We next analyzed axonal injury by comparing the percent area of neurofilament protein 200 (NF200) in both ventral and dorsal regions. Males showed a decreasing trend of NF200 positive area with age in both regions, but axon injury was most pronounced in age and diseased males. Neuronal counts were measured via NeuN staining in both ventral and dorsal horns. We found a decrease in neuron counts at young EAE and midlife EAE, but no effect of aging. Together this demonstrates the classical signs of demyelination, axon injury, and neuronal loss with disease in our EAE induced mice. This also reveals an effect of age on myelin and axonal integrity.

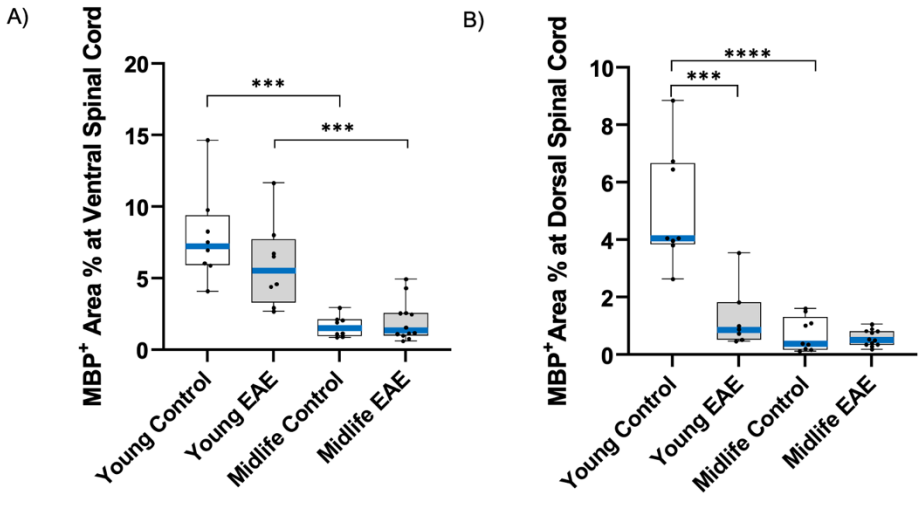

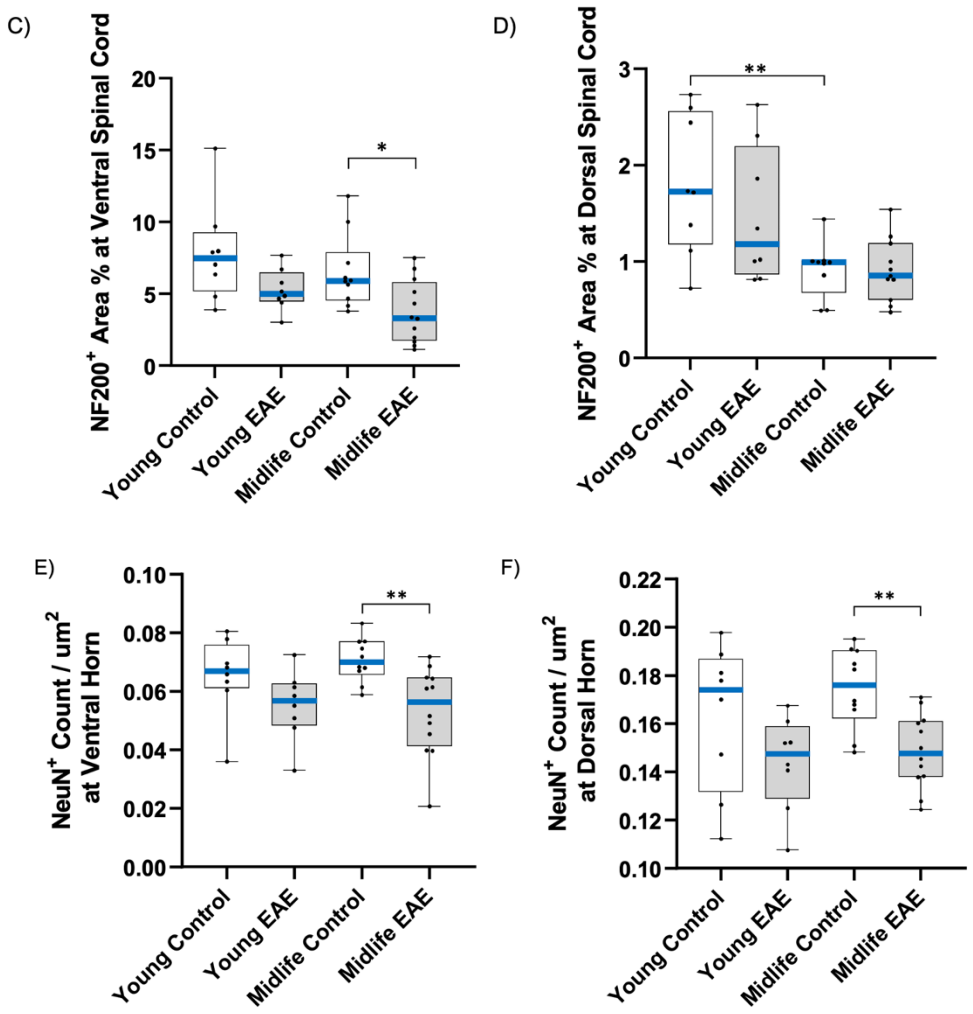

Figure 2: Myelin, axonal, and neuronal changes in aging EAE. (A) Quantification of myelin basic protein (MBP) positive labeled area fraction in ventral spinal cord (male). A decrease in MBP protein expression was shown in midlife control and midlife EAE. (B) Quantification of MBP protein expression in dorsal spinal cord measured as an area fraction. Significant decrease in MBP protein expression with aging when compared to controls. (C) NF200 protein expression in ventral spinal cord measured by positive labeled area fraction. NF200 was shown to slightly decrease at midlife EAE. (D) NF200 protein expression in dorsal spinal cord. NF200 area decreased with aging. (E) NeuN positive counts at ventral horn are significantly decreased at midlife EAE compared to their aged controls. (F) NeuN positive counts at dorsal horn are significantly decreased in midlife EAE compared to aged controls. All male spinal cords. Median bars are highlighted in blue. *P < 0.05, **P < 0.01, ***P < 0.001, ****P < 0.0001.

Midlife mice had reactive astrogliosis in thalamus

Our neuropathology analysis began with investigating astrocyte activation in the thalamus. The colocalization of astrocytes and inflammatory biomarkers was shown at the protein level via immunohistochemistry using GFAP and LCN2 labeling. The double positive

LCN2 and GFAP area revealed increased astrocyte activation in both male and female mice with aging. Both male and female young groups had very low double positive area fractions. Females showed a significant increase in LCN2+ GFAP+ area % in thalamus at midlife control and midlife EAE. Males also revealed significant microglia activation at midlife control and midlife EAE compared to their young control and young EAE. Interestingly males revealed greater double positive labeling demonstrating further astrocyte activation at midlife EAE in a disease by age interaction.

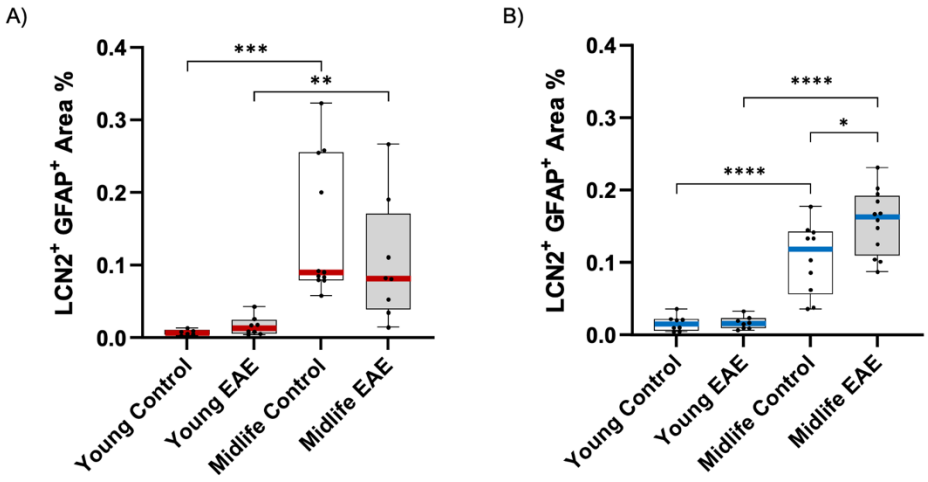

Figure 3: Thalamic reactive astrogliosis in aging EAE. (A) Colocalized area fraction quantifying astrocyte activation in female thalamus. Double positive GFAP LCN2 area fraction was shown to increase with aging and EAE. Significant increase in midlife control and midlife EAE when compared to their age matched mice. (B) Colocalized area fraction quantifying astrocyte activation in male thalamus. LCN2 GFAP positive area fraction increased with aging. There was greater astrocyte activation in midlife EAE compared to midlife control. Median bars are highlighted in red (female) and blue (male). *P < 0.05, **P < 0.01, ***P < 0.001, ****P < 0.0001.

Midlife mice had reactive microgliosis in thalamus

Next, we investigated the resident immune cells of the CNS. The colocalization of macrophage marker Iba1 and antigen presenting cell specific immune response marker MHCII shows microglia activation. The double positive area fraction divided by the Iba1+ area fraction is specifically looking at the activated microglia. In females we see an increase in microglia activation in midlife control as well as midlife EAE at the thalamus. In males we also have a

significant increase of microglia activation in midlife control and midlife EAE. We then looked at the morphology of microglia in the thalamus. We measured the Iba1+ area and the perimeter. The morphology is more of a representation of the microglia's functional state. The "resting" state has a smaller area to perimeter fraction, while the activated state has a larger ratio. Perimeters were increased with aging in both females and males, regardless of whether or not they have EAE (Segal, 2022). Also, we analyzed the resting state of microglia in the thalamus using the homeostatic marker P2RY12. The thalamus showed a trend for a decrease in resting microglia (P2RY12 area fraction) in both males and females with aging, consistent with observations of an increase in activated microglia.

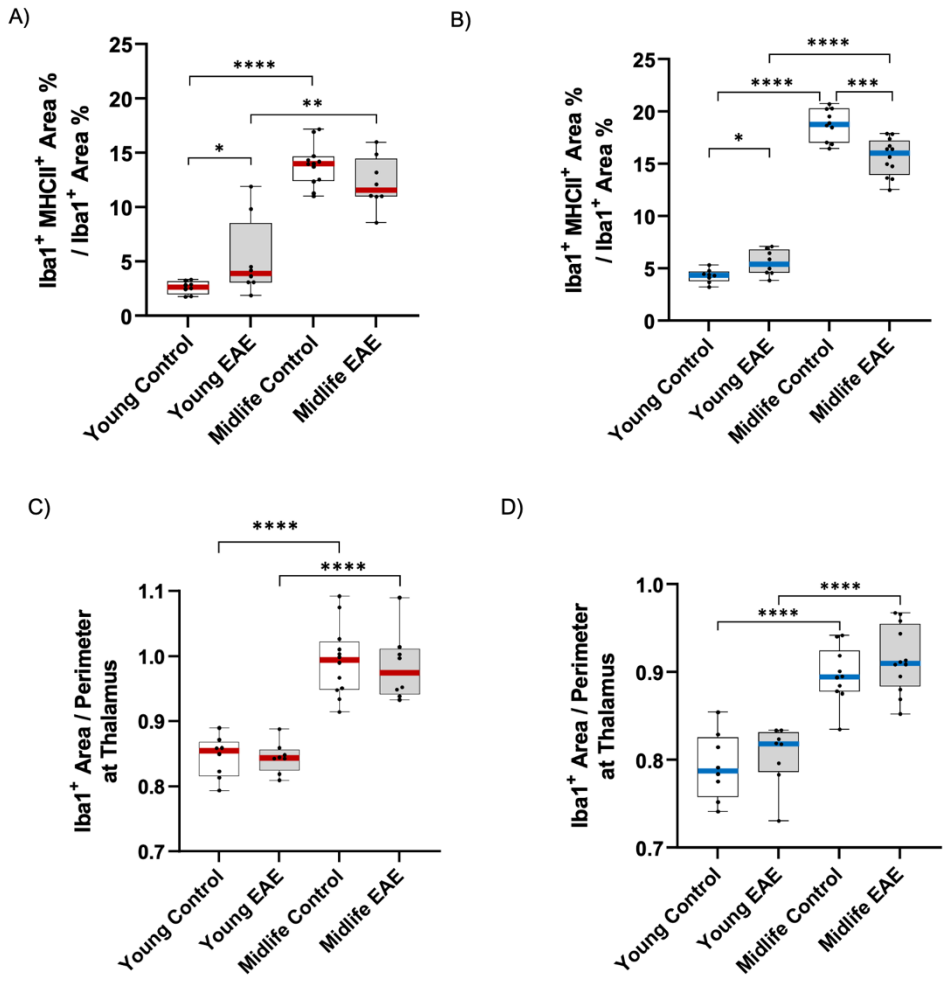

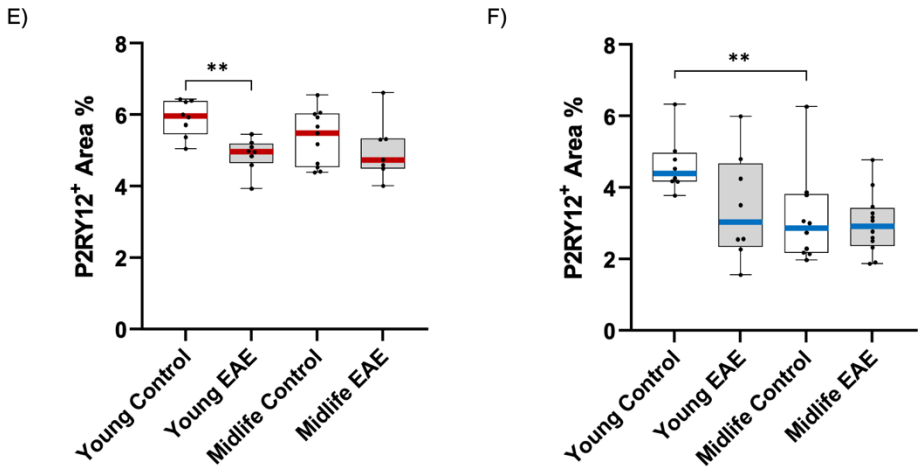

Figure 4: Microglia activation, morphology, and homeostatic changes in aging EAE. (A) Quantification of microglia activation in female thalamus via Iba1 MHCII protein expression. Colocalized area fraction in Iba1 positive area specifically represents activated microglia. Significant increase in activation in midlife control and midlife EAE. (B) Quantification of microglia activation in male thalamus via Iba1 MHCII protein expression. Double positive area fraction significantly increased with aging. (C) Female microglia morphology. The measured area and perimeter ratio was used to quantify microglia activation state. Greater area to perimeter ratio in midlife control and midlife EAE shows greater activation at female thalamus. (D) Male microglia morphology. Area to perimeter ratio quantified activation state. Greater ratio in midlife EAE and midlife control. (E) Homeostatic microglia quantification via P2RY12 protein expression. Decreased area fraction in disease compared to healthy control demonstrates lower resting microglia in female thalamus. (F) Homeostatic microglia quantification via P2RY12 protein expression showed significant area fraction decrease with aging in midlife EAE. Median bars are highlighted in red (female) and blue (male). *P < 0.05, **P < 0.01, ***P < 0.001, ****P < 0.0001.

Midlife mice had post-synaptic loss in thalamus

Lastly, we investigated synaptic loss in the thalamus. Microglia have multiple roles in the CNS and are never "resting" instead they continue to survey and maintain homeostasis by neuromodulation and phagocytosis. Microglia greatly contribute to synaptic circuits via synaptic pruning, debris phagocytosis, and secretion of multiple neurotrophic factors. We investigated the presynaptic and postsynaptic densities at the protein level via immunohistochemistry labeling SYN1 and PSD95. Synaptic networks in the thalamus showed changes postsynaptically. PSD95 area fractions decreased in both males and females at midlife control and midlife EAE. Presynaptic terminals had no significant changes across all groups in both males and females. Finally, the colocalization of SYN1 and PSD95 was decreased in aged midlife control and aged midlife EAE.

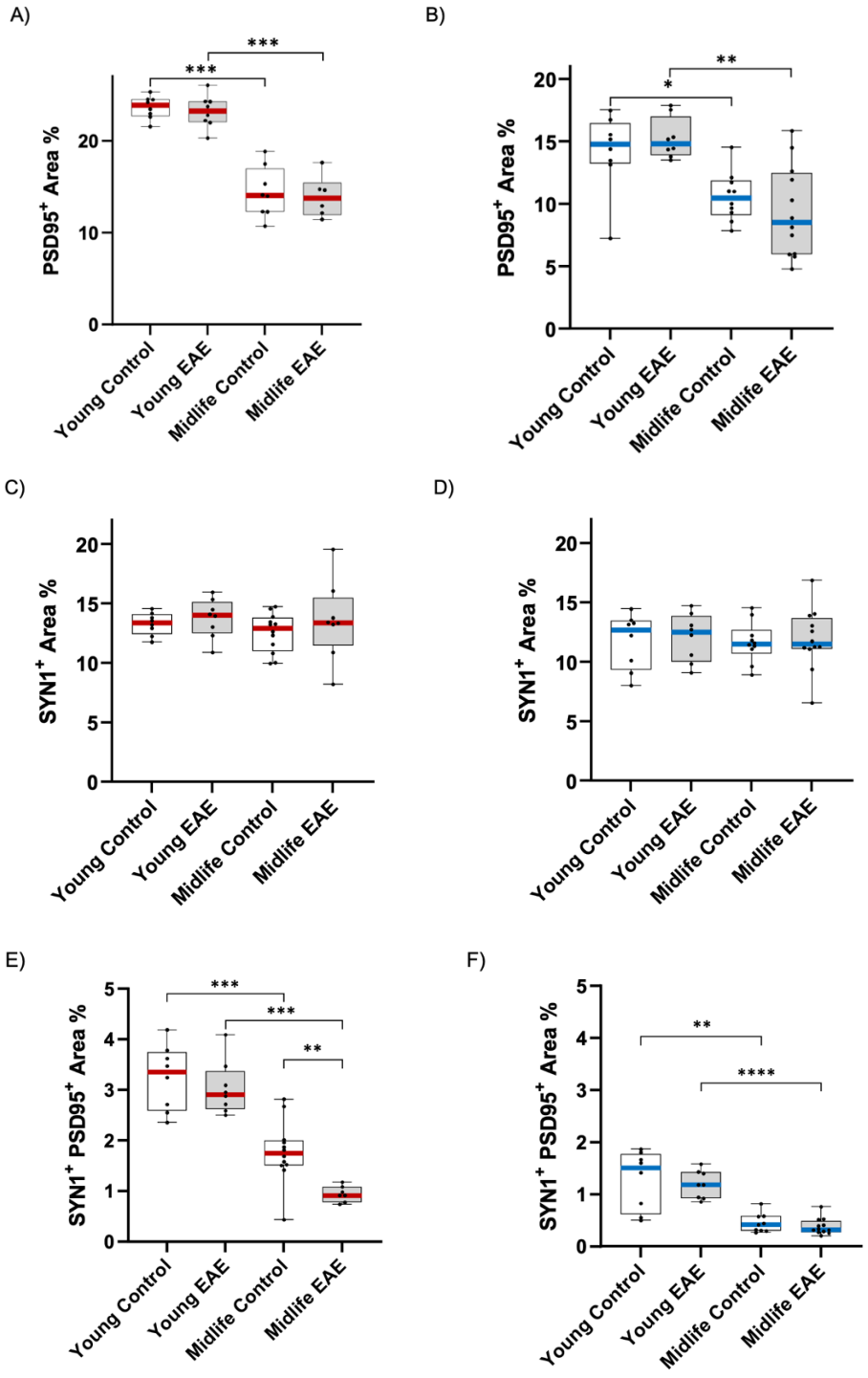

Figure 5: Pre- and post-synaptic changes in aging EAE. (A) Postsynaptic quantification via PSD95 protein expression. Female thalamus had decrease in PSD95 area fraction in midlife control and midlife EAE. (B) Postsynaptic quantification via PSD95 protein expression. Male thalamus had decrease in PSD95 area fraction with aging and even greater decrease with disease as shown in midlife EAE. (C) Presynaptic quantification via SYN1 protein expression. No changes in female thalamus. (D) Presynaptic quantification in male thalamus. No significant changes across all groups. (E) Colocalized area fraction in female thalamus. Decrease synaptic area in midlife control and midlife EAE. (F) Colocalized area fraction in male thalamus. Significant decrease in synaptic area at midlife control and midlife EAE. Median bars are highlighted in red (female) and blue (male). *P < 0.05, **P < 0.01, ***P < 0.001, ****P < 0.0001.

Discussion:

The role of biological aging in thalamic network injury seen in EAE and MS was assessed via direct comparisons in aged control and disease mice. The thalamus is a critical region related to motor and sensory networks, as well as associated nuclei that affect cognition and vision. The variety of disabilities that manifest from CNS lesions are highly connected through thalamic nuclei, the central relay center. Our experiment revealed significant microglia and astrocyte activation, as well as postsynaptic loss in thalamic grey matter atrophy. Our findings show age as the most significant factor, but other factors can contribute. Future studies investigating specific thalamic nuclei can reveal insights into the effect of aging on specific disabilities that progress in MS in women and men.

Materials and Methods

Mice Procedure Guidelines:

Animals were maintained under standard conditions in a 12-h dark/light cycle with free access to food and water ad libitum. All procedures were done in accordance with the guidelines of the National Institutes of Health and the Chancellor's Animal Research Committee the University of California, Los Angeles Office for the Protection of Research Subjects.

Active EAE Induction, Clinical Scoring, and Treatment:

Male and female wildtype mice were induced with active EAE as described previously for C57BL/6J mice (5). Briefly, young male and female, age 8- to 12-wk-old, and midlife male and female, age 52- to 60-wk-old mice were injected s.c. with myelin oligodendrocyte glycoprotein (MOG) amino acids 35 to 55 (200μg per animal; Mimotopes) emulsified in complete Freund's adjuvant, supplemented with Mycobacterium tuberculosis H37Ra (200μg per animal; Difco Laboratories), over two sites drained by left inguinal and axillary lymph nodes in a volume of 0.1mL per mouse. One Week later, a booster immunization was applied s.c., over contralateral lymph nodes. Pertussis Toxin (500ng per mouse; List Biological Laboratories, Inc.) was injected intraperitoneally on days 0 and 2 (6). The animals were monitored daily for EAE signs based on a standard EAE 0 to 5 scale scoring system as follows: 0, healthy; 1, complete loss of tail tonicity; 2, loss of righting reflex; 3, partial paralysis; 4, complete paralysis of one or both hind limbs; and 5, premoribund state, as described (7). For higher scoring mice treatment included daily s.c. injections of lactated ringer's solution to replenish fluids and electrolytes, clear H_2O

recovery diet gel for nourishment, triple antibiotic ointment, and heat pads to help maintain core body temperature.

Immunohistochemistry:

Mice were deeply anesthetized in isoflurane and perfused transcardially with ice-cold 1×PBS for 20 to 30 minutes, followed by 4% paraformaldehyde for 10 to 15 minutes. CNS tissues were dissected and submerged in 10% formalin overnight at 4°C, followed by 30% sucrose for 24h. Spinal cords were cut in thirds and embedded in an optimal cutting temperature (OCT) compound and stored at −80°C after being flash-frozen by dry ice. The 40-µm thick free-floating spinal cord cross-sections were prepared using a cryostat (Leica Biosystems) at −20°C. Tissues were collected serially and stored in 1×PBS with 0.1% sodium azide at 4°C. Whole brains were flat-embedded in OCT compound and flash-frozen using dry ice. Following embedding, 40-µm thick sagittal sections were cut using a cryostat at −20°C. Tissues were collected serially and stored in 1×PBS with 0.1% sodium azide at 4°C until further use. Both spinal cord and brain sections were placed in their respective wells before histological staining and stored at 4°C. 40-µm thick brain and spinal cord free-floating sections were thoroughly washed with 1×PBS to remove residual sodium azide, followed by a one time 50% methanol wash. Post-fixed tissue antigen detection was improved using heat-induced antigen retrieval by washing sections with microwaved 10mM Citric Acid - 0.05% Tween 20 followed by 1×PBS washing. All tissue sections were permeabilized on ice with 0.5% Triton X-100 in 1×PBST for 15 minutes and thoroughly washed with 1×PBST. Brain and spinal cord sections were incubated with a 10% normal goat serum in 1×PBST blocking buffer for 1 hour at room temperature. Tissues were then incubated with primary antibodies over the weekend at 4°C. After the 72 hour incubation, the

tissues are thoroughly washed and incubated with secondary antibodies conjugated with Cy5 or Cy3 at 1:500 (Millipore) in 2% normal goat serum and 1×PBST for 2 hours at room temperature. Sections were mounted onto microscope slides (Super frost plus; VWR), allowed to semi-dry, coverslipped in fluoromount G (SouthernBiotech) and sealed for confocal microscopy. The following primary antibodies were used to investigate MS pathology for microgliosis, astrogliosis, and synaptic plasticity. Microgliosis with *Ionized calcium-binding molecule 1* / **Iba1**: rabbit anti-Iba1 (at 1:500; Fujifilm/Wako), *Major histocompatibility complex class II* / **MHC class II**: rat anti-MHCII (at 1:500; BioLegend), *Purinergic receptor P2Y12* / **P2RY12**: rat anti-P2RY12 (at 1:100; BioLegend), and *Dectin-1* / **Clec7a**: rabbit anti-Clec7a (at 1:200; Invitrogen). Astrogliosis with *Lipocalin-2* / **LCN2**: goat anti-LCN2 (at 1:50; Bio-Techne R&D systems), and *Glial fibrillary acidic protein* / **GFAP**: rat anti-GFAP (at 1:500; Invitrogen). Synaptic plasticity with *Synapsin-1* **SYN1**: rabbit anti-SYN1 (at 1:500; Synaptic Systems), *Postsynaptic density protein-95* / **PSD95**: guinea pig anti-PSD95 (at 1:250; Synaptic Systems), *Vesicular glutamate transporter-2* / **VGluT2**: guinea pig anti-VGluT2 (at 1:1000; Millipore), and *Postsynaptic density protein-95* / **PSD95**: rabbit anti-PSD95 (at 1:200; ThermoFisher).

Image Analysis:

Through the use of immunohistochemistry, we labeled proteins of interest that assist us in analyzing glial cells as well as synapses in the MS animal model, EAE. To begin analyzing our confocal images we import our labeled image into FIJI and split each channel. Once all of our channels have been split, we proceed to create a "Max Intensity" image for each channel using the *z projection* function in FIJI and we save our new max intensity images. To further clean up our image we use the *subtract background* function in FIJI by selecting a rolling ball radius

based on pixel size. Find a radius that will remove the background noise and sharpen the features that we are analyzing. The purpose of reducing background is to make our signal more pronounced in order to create a clearer binary representation. Using the subtracted background image we just created we apply the *auto threshold* function to produce a binary image from a method that best fits our channel and structures.

With our max intensity images, and auto threshold images we will create a region of interest (ROI) for each channel. In the case of Iba1 we create ROI's and save each one as an overlay, and we do the same for MHC2. In order to produce colocalized ROI we use one of the channel binary images with ROI as an overlay, and in the ROI manager we import the opposite channel's ROI. Using the *and* function in ROI manager we can create a colocalized ROI where we have signal from both channels. Occasionally our slides have air bubbles, so using the ROI feature we are able to exclude regions that contain air bubbles, but also to ensure we only include the brain regions we are interested in such as the thalamus.

In order to produce area fractions, we need to measure the total area found within the thalamic region for each image. In FIJI we use the binary image with the thalamus ROI overlay to measure the area. We then take area measurements for the colocalized area (Iba1+ and MHC2+), each channel individually (Iba1+ or MHC2+), as well as mean intensity values for both channels. From FIJI we are able to export the data as 'csv' files and export to excel. Once in excel we create our area fraction such as (Iba1+ Area)/ (Total CA1 Area) represented as a percentage. All values are averaged for each animal and saved for Data Analysis based on experimental groups.

Statistical Analysis:

All analyses were done in a blinded fashion. Data are means ± SEM with error bars representing biological variability between mice within each group. Data distribution was assumed to be normal. Sample sizes were designed with adequate power according to the literature and our previous studies. Statistical analyses of protein expression changes in EAE were performed with t-test and two way-ANOVA using Prism 6 (version 6.0h) software (GraphPad).

Acknowledgements:

This work was supported by the National Institutes of Health (NIH) grants: R35NS132150, R01NS096748 and R01NS109670 to R.R.V.

Special thanks to Dr. Noriko Itoh who performed the clinical EAE induction studies, as well as to Nadya Higgins for assistance with immunohistochemistry, confocal imaging, and analysis of brain and spinal cord sections.

References

Gh Popescu, B. F., & Lucchinetti, C. F. (2012, March 7). Meningeal and cortical grey matter pathology in multiple sclerosis - BMC neurology. BioMed Central.

Garg, N., & Smith, T. W. (2015, August 3). An update on immunopathogenesis, diagnosis, and treatment of multiple sclerosis. Wiley Online Library.

Voskuhl RR, Itoh N, Tassoni A, Matsukawa MA, Ren E, Tse V, Jang E, Suen TT, Itoh Y. Gene expression in oligodendrocytes during remyelination reveals cholesterol homeostasis as a therapeutic target in multiple sclerosis. Proc Natl Acad Sci U S A. 2019.

Tassoni A, Farkhondeh V, Itoh Y, Itoh N, Sofroniew MV, Voskuhl RR. The astrocyte transcriptome in EAE optic neuritis shows complement activation and reveals a sex difference in astrocytic C3 expression. Sci Rep. 2019;9(1):10010.

Itoh N, Itoh Y, Tassoni A, Ren E, Kaito M, Ohno A, Ao Y, Farkhondeh V, Johnsonbaugh H, Burda J, Sofroniew MV, Voskuhl RR. Cell-specific and region-specific transcriptomics in the multiple sclerosis model: Focus on astrocytes. Proc Natl Acad Sci U S A. 2018;115(2):E302-E9.

Voskuhl RR. The effect of sex on multiple sclerosis risk and disease progression. Mult Scler. 2020;26(5):554-60. Epub 2020/01/23. doi: 10.1177/1352458519892491. PubMed PMID: 31965884; PMCID: PMC7160019.

Voskuhl RR, Gold SM. Sex-related factors in multiple sclerosis susceptibility and progression. Nat Rev Neurol. 2012;8(5):255-63. Epub 2012/03/28. doi: 10.1038/nrneurol.2012.43 nrneurol.2012.43 [pii]. PubMed PMID: 22450508; PMCID: 4435786.

Ortona E;Pierdominici M;Maselli A;Veroni C;Aloisi F;Shoenfeld Y; (n.d.). Sex-based differences in autoimmune diseases. Annali dell'Istituto superiore di sanita.

Eshaghi, A., et al. Progression of regional grey matter atrophy in multiple sclerosis. Brain 141, 1665-1677 (2018).

Bergsland, N., et al. Subcortical and cortical gray matter atrophy in a large sample of patients with clinically isolated syndrome and early relapsing-remitting multiple sclerosis. AJNR Am J Neuroradiol 33, 1573-1578 (2012).

Voskuhl, R.R., et al. Sex differences in brain atrophy in multiple sclerosis. Biol Sex Differ 11, 49 (2020).

Eshaghi, A., et al. Deep gray matter volume loss drives disability worsening in multiple sclerosis. Ann Neurol 83, 210-222 (2018).

Hughes, E.J., et al. Regional changes in thalamic shape and volume with increasing age. Neuroimage. 63, 1134-1142 (2012).

Wang, Y., Xu, Q., Luo, J., Hu, M. & Zuo, C. Effects of Age and Sex on Subcortical Volumes. Front Aging Neurosci 11, 259 (2019).

Hanninen, K., et al. Thalamic Atrophy Predicts 5-Year Disability Progression in Multiple Sclerosis. Front Neurol 11, 606 (2020).

Magon, S., et al. Volume loss in the deep gray matter and thalamic subnuclei: a longitudinal study on disability progression in multiple sclerosis. J Neurol 267, 1536-1546 (2020).

Amin, M. & Ontaneda, D. Thalamic Injury and Cognition in Multiple Sclerosis. Front Neurol 11, 623914 (2020).

Minagar, A., et al. The thalamus and multiple sclerosis: modern views on pathologic, imaging, and clinical aspects. Neurology 80, 210-219 (2013).

Iglesias, J.E., et al. A probabilistic atlas of the human thalamic nuclei combining ex vivo MRI and histology. Neuroimage 183, 314-326 (2018).

Cerri, S., et al. A contrast-adaptive method for simultaneous whole-brain and lesion segmentation in multiple sclerosis. Neuroimage 225, 117471 (2021).

MacKenzie-Graham A, et al. (2009) Purkinje cell loss in experimental autoimmune encephalomyelitis. Neuroimage 48:637–651.

Nisticò R, et al. (2013) Inflammation subverts hippocampal synaptic plasticity in experimental multiple sclerosis. PLoS One 8: e54666

Bakshi R, Benedict RH, Bermel RA, Jacobs L. Regional brain atrophy is associated with physical disability in multiple sclerosis: semiquantitative magnetic resonance imaging and relationship to clinical findings. J Neuroimaging. 2001;11(2):129–36

Morgen K, Sammer G, Courtney SM, Wolters T, Melchior H, Blecker CR, et al. Evidence for a direct association between cortical atrophy and cognitive impairment in relapsing-remitting MS. Neuroimage. 2006;30(3):891–8

Prinster A, Quarantelli M, Lanzillo R, Orefice G, Vacca G, Carotenuto B, et al. A voxel-based morphometry study of disease severity correlates in relapsing—remitting multiple sclerosis. Mult Scler. 2010;16(1):45–54

MacKenzie-Graham A, Kurth F, Itoh Y, Wang HJ, Montag MJ, Elashoff R, et al. Disability-specific atlases of gray matter loss in relapsing-remitting multiple sclerosis. JAMA Neurol. 2016;73(8):944–53

Deborah L. Smith-Bouvier, Anagha A. Divekar, Manda Sasidhar, Sienmi Du, Seema K. Tiwari-Woodruff, Jennifer K. King, Arthur P. Arnold, Ram Raj Singh, Rhonda R. Voskuhl; A role for sex chromosome complement in the female bias in autoimmune disease. *J Exp Med* 12 May 2008; 205 (5): 1099–1108.

Sienmi Du, S. Du, Noriko Itoh, N. Itoh, Sahar Askarinam, S. Askarinam, Haley Hill, H. Hill, Arthur P. Arnold, A. P. Arnold, & Rhonda R. Voskuhl, R. R. Voskuhl. (0000). XY sex chromosome complement, compared with XX, in the CNS confers greater neurodegeneration during experimental autoimmune encephalomyelitis. *Proceedings of the National Academy of Sciences of the United States of America, 111*, 2806-2811.

Atkinson JR, Jerome AD, Sas AR, Munie A, Wang C, Ma A, Arnold WD, Segal BM. Biological aging of CNS-resident cells alters the clinical course and immunopathology of autoimmune demyelinating disease. JCI Insight. 2022 Jun 22;7(12):e158153. doi: 10.1172/jci.insight.158153. PMID: 35511417; PMCID: PMC9309055.